

Analysis of the Influence of Diode Reverse Recovery on the Operation and Design of High-Frequency Rectifiers

Љupčo V. Karadžinov, *Member, IEEE* and David C. Hamill, *Senior Member, IEEE*,

Abstract—Diode reverse recovery can cause anomalies in high-frequency rectifier operation, including self-sustaining quasiperiodic oscillations. The output voltage can increase considerably beyond that predicted by the usual analysis. This nonlinear effect is analyzed using a recently developed piecewise-linear diode model. The theoretical results agree with experimental measurements. Design guidelines are presented to avoid overvoltage and instability in practical converters.

Index Terms—Design constraints, DH phenomenon, diodes, nonlinear dynamics, rectification, reverse recovery, series-resonant converters.

I. INTRODUCTION

RECENT YEARS have seen a push toward ever higher switching frequencies, with the aim of reducing the volume and mass of power converters. At high frequencies, unavoidable parasitic capacitances and inductances dominate the circuit action, leading to unacceptable switching loss and inefficiency. The question naturally arises: Do the inherent limitations of practical components and parasitic elements impose an upper limit on the usable switching frequency? In attempting an answer, much attention has been paid to resonant and quasiresonant converter topologies; to the switching devices and their drive circuits; and to transformers and inductors. To date, however, little work has been done to establish the effect of nonideal rectifier diodes, which play an essential role in power converters, especially those with a dc output. One reason may be the inherent nonlinearity of diodes, which gives rise to intractable equations, precluding helpful analysis.

In this paper we investigate the interaction between intentional or parasitic inductance and the reverse recovery of nonideal diodes, an essentially nonlinear process. We find anomalous behavior which causes significant output overvoltage and quasiperiodic oscillations.

PWM and resonant switching converters operating at high switching frequencies have complex voltage and current waveforms. This necessitates the use of many approximations in their analysis [1]–[5]. The most common is the use of ideal

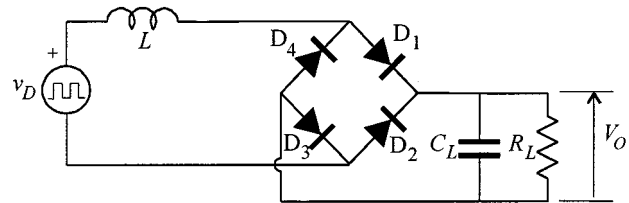


Fig. 1. Class D bridge rectifier with inductive drive.

switches as models for the semiconductor devices. For resonant converters, to further simplify the analysis and design, the fundamental-component method is frequently used [3], [5]. This gives good results when the loaded Q factor is high and the switching frequency is close to the resonant frequency. However, such an analysis cannot predict all effects, some of which can cause the practical circuit to exhibit unexpected and sometimes strange behavior.

In this paper we are concerned with the phenomenon of increased output voltage in a high-frequency bridge rectifier fed by an inductive source, as shown in Fig. 1. This rectifier (or similar) forms part of many power converters. The inductance L can be introduced intentionally, or it can come from leakage and stray inductances. In particular, it forms an essential part of the series-resonant converter, Fig. 2, where this effect was first noticed [6]. Analyzing these converters assuming ideal switches, explicit equations can be obtained for the output voltage V_O . According to these equations, the output voltage is always lower than the input drive voltage v_D [3], [5]. However, in practical converters with certain circuit parameters, e.g., when the rectifier circuit employs slow power diodes or has light loading, there are considerable deviations from ideal operation.

These deviations are clearly depicted in Fig. 3, which shows how the measured output voltage depends on the drive frequency. Fig. 3 uses the series-resonant converter model of Fig. 4 with the following parameters: v_D is a square-wave generator with high and low voltage levels $\pm V_D = \pm 5$ V, $L = 9.42$ mH, $C_R = 23.2$ nF, four diodes MR752 with storage delay time $t_{sd} = 5$ μ s (or minority carriers lifetime $\tau = 7.2$ μ s), $C_L = 61.5$ nF and load $R_L = 10$ k Ω . Above the resonant frequency $f_0 = 10.766$ kHz, the output voltage rises. At 45 kHz it reaches its maximum: 2.4 times that predicted by analysis, $V_{Dpk-pk}/2$. At frequencies below the maximum, the output voltage oscillates between two levels, depicted by two lines in Fig. 3.

Manuscript received July 14, 1998; revised August 2, 1999. Recommended by Associate Editor, W. Portnoy.

L. V. Karadžinov is with the Faculty of Electrical Engineering, SS. Cyril and Methodius University, Skopje 91000, Macedonia (e-mail: l.karadzinov@ieee.org).

D. C. Hamill is with the Surrey Space Centre, University of Surrey, Guildford, Surrey GU2 5XH, U.K. (e-mail: d.hamill@surrey.ac.uk).

Publisher Item Identifier S 0885-8993(00)02332-2.

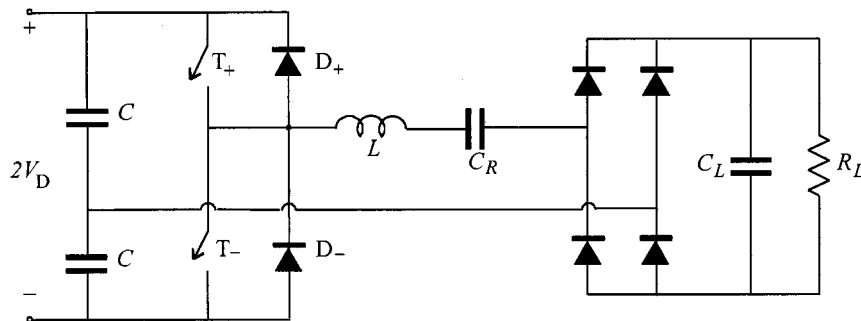


Fig. 2. Series-resonant converter (SRC).

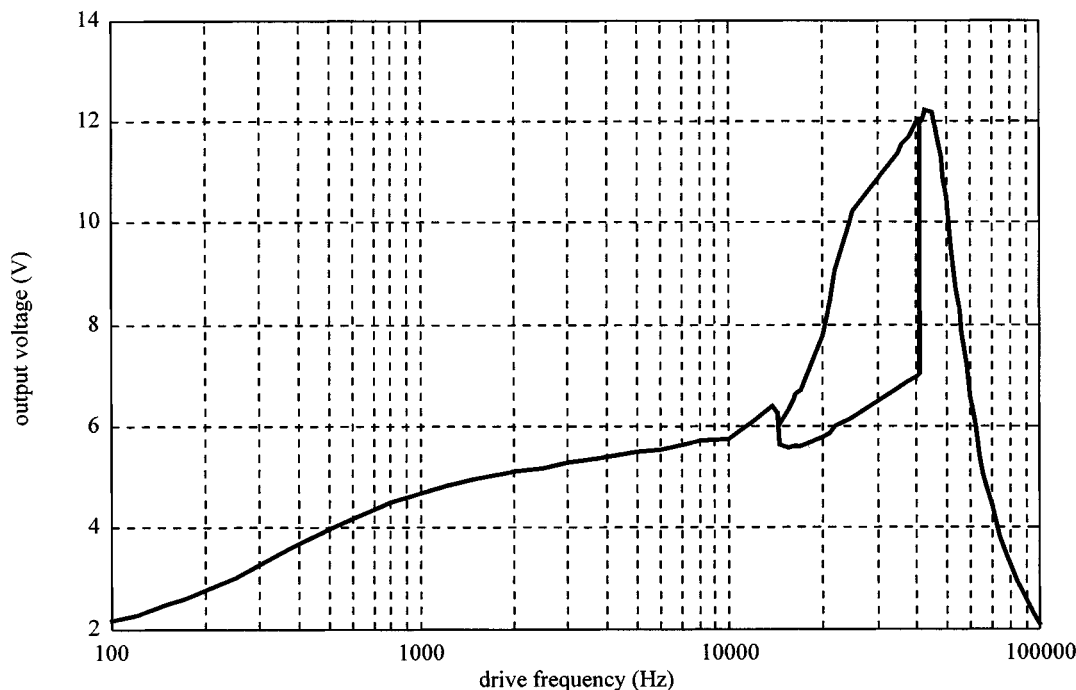


Fig. 3. Measured deviations from ideal operation of the SRC. The output voltage is considerably higher than that predicted by analysis. From 14–41 kHz, the output voltage oscillates between two levels.

These diodes were selected to permit a conveniently low test frequency. One would not normally use such slow diodes in a practical converter; however, it will be shown that the results are scalable. Thus if the component values are suitably altered for higher frequency operation, the same overvoltage peak is expected to appear at 450 kHz with 500 ns diodes (“fast recovery”), and at 4.5 MHz with 50 ns diodes (“ultra-fast recovery”).

This oscillation was first described by Deane and Hamill [6] and was subsequently named the *DH phenomenon* [8], [9]. Fig. 5 shows the bridge rectifier’s input voltage. This square-wave voltage appears amplitude-modulated at a frequency apparently unrelated to the switching frequency (quasiperiodicity). The output voltage follows the envelope of the bridge voltage and thus has the same modulation. This might cause the converter to malfunction, especially if it enters a control loop.

The above behavior is quite robust: it exists for a wide range of circuit parameters and with different diode types. For ex-

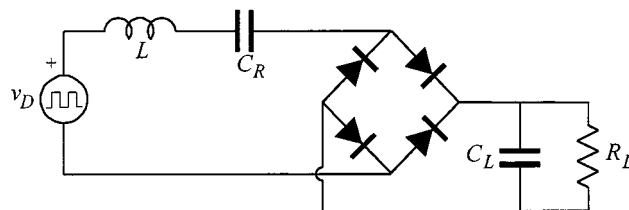


Fig. 4. Model of the series-resonant converter.

ample, computer simulations of the DH phenomenon [7], [9] show that it depends only slightly on the capacitance C_R in the series resonant circuit. Even if C_R is absent, i.e., if we have the circuit of Fig. 1, the phenomenon is present in the circuit with its full complexity, as shown in Fig. 6. The only difference is that the voltage dependence on frequency is flat below resonance. Deane and Hamill [6] found that this behavior is caused by the diodes’ nonlinear transient characteristics, e.g., reverse recovery. Similar effects occur frequently in practice, but they

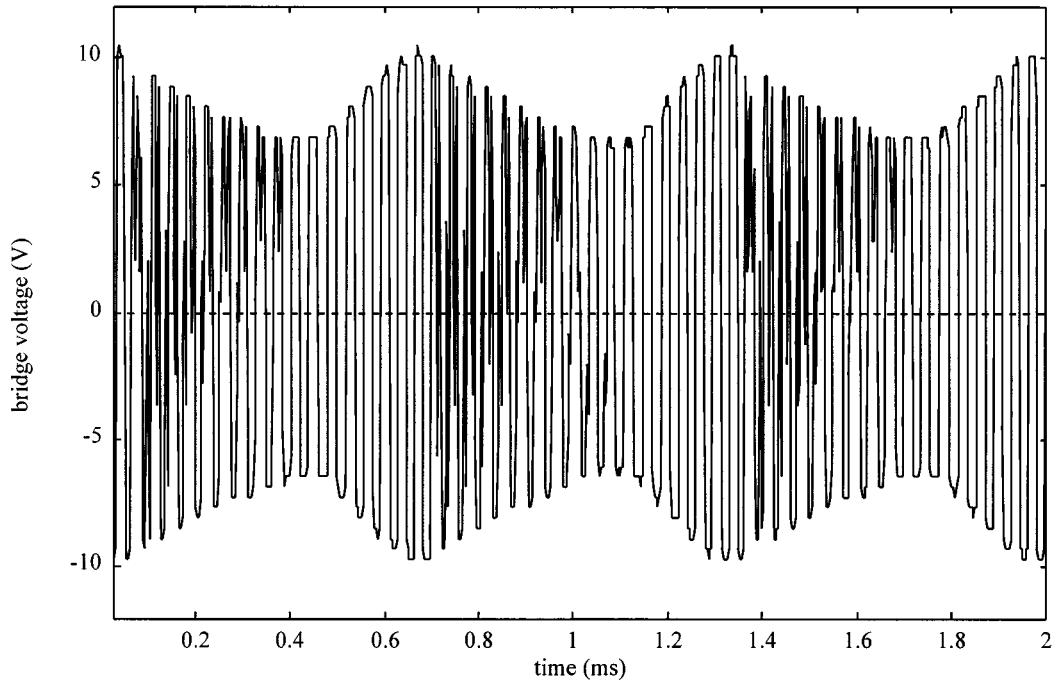


Fig. 5. DH phenomenon in series-resonant converter: case when $f = 27$ kHz.

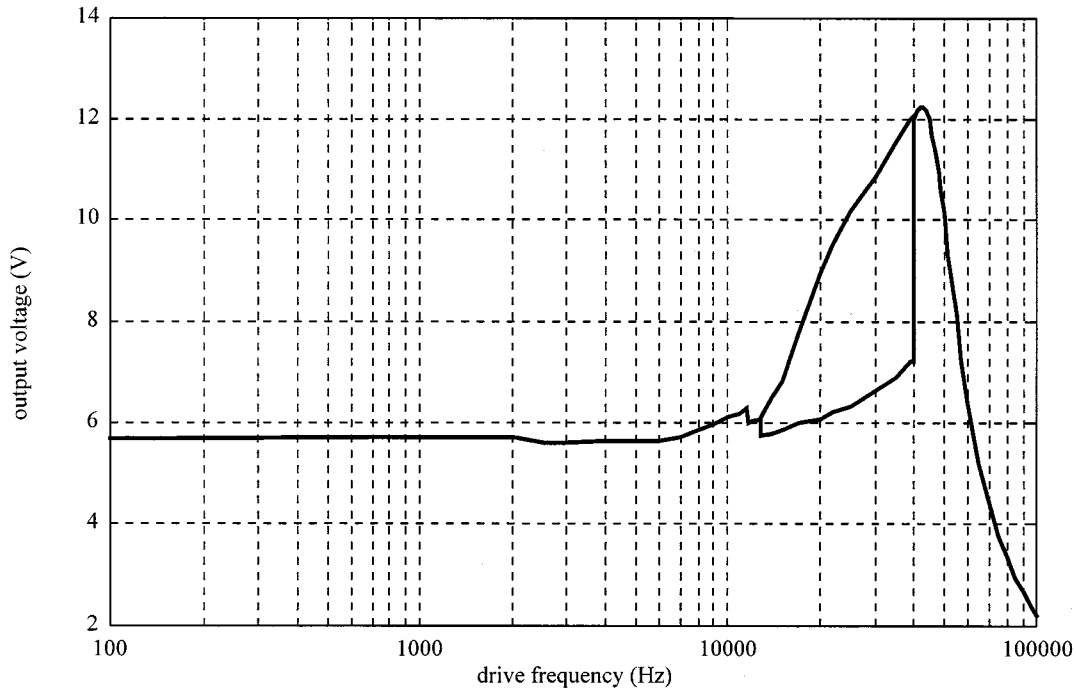


Fig. 6. Measured output voltage dependence on the drive frequency in the circuit of Fig. 1.

are rarely reported in the literature and, to the best of our knowledge, no analysis has been presented to date.

In this paper we analyze the influence of reverse recovery on the operation of bridge rectifiers, and determine design constraints to prevent these effects. Until recently, the main obstacle to analysis has been the lack of an appropriate diode model: one that is not only simple enough to allow analysis but is also ac-

curate enough to reveal the observed phenomena. For example, PSpice and SABER contain elaborate models of diodes that are good for simulation, but are too complex for mathematical analysis. Recently, however, a suitable piecewise-linear (PWL) diode model has been developed [8]. This model, used in our analysis, is shown in Fig. 7. It comprises two linear capacitances, a linear resistance, and an ideal switch, whose state de-

depends on the anode–cathode voltage. The PWL model is capable of modeling, to first order, transient effects such as reverse recovery.

In Section II we analyze a bridge rectifier fed from an inductive source, assuming ideal diodes. This provides a baseline for the more detailed analysis of Section III, which employs a diode model with reverse recovery. The resulting nonlinear equations are solved numerically, and the results are presented as normalized graphs in Section IV. We end with a discussion of design issues in Section V and draw some conclusions in Section VI.

It turns out that there are two important nondimensional parameters. First we have $A = \tau R_L/L$, which expresses the diodes' minority carrier recombination time τ as a multiple of the circuit's L/R_L time constant. Anomalous phenomena occur when A exceeds unity: this can always happen if R_L is made large enough. Second is the normalized switching period, $T_n = T/\tau$, where T is actual switching period. Because these two parameters A and T_n are dimensionless, it can be deduced that the effects seen at low frequencies with slow diodes will also appear at high frequencies with fast diodes.

II. IDEAL OPERATION

For comparison purposes, we first analyze ideal operation of the rectifier in Fig. 1. The filter capacitor C_L at the output is assumed to be very large, as normal in applications requiring a nearly constant instantaneous output voltage $v_O \approx V_O$. The drive voltage v_D is a square wave with amplitude $\pm V_D$ and period T . The diodes are modeled initially as ideal switches which turn on and off instantaneously.

Inductor current i_L and voltage v_L waveforms are shown in Fig. 8. Under steady-state conditions, these waveforms are symmetrical with respect to zero and have equal peak values $|I_{L\text{MAX}}| = |I_{L\text{MIN}}|$ (i.e., area A is equal to area B). This gives

$$\frac{V_D + V_O}{L} \cdot T_1 = \frac{V_D - V_O}{L} \cdot \left(\frac{T}{2} - T_1 \right).$$

This equation has two unknowns, V_O and T_1 . Time interval T_1 is the time needed for the current i_L to drop to zero and is also the delay time of the bridge pulses. The second equation needed for determining these unknowns is obtained from the output stage of the converter

$$V_O = R_L \cdot I_O = R_L \cdot \frac{I_{L\text{MAX}}}{2}$$

where $I_{L\text{MAX}} = \frac{V_D + V_O}{L} \cdot T_1$.

After some algebra, we obtain the following expressions in V_O and T_1 :

$$\frac{V_O}{V_D} = -\frac{4L}{R_L T} + \sqrt{\left(\frac{4L}{R_L T} \right)^2 + 1} \quad (1)$$

$$T_1 = \frac{2L}{R_L} \cdot \frac{V_O/V_D}{V_O/V_D + 1}. \quad (2)$$

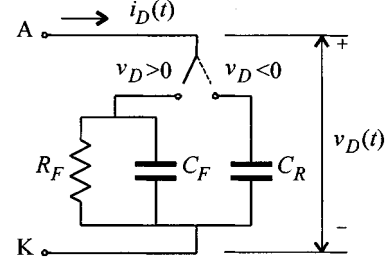


Fig. 7. Simplest PWL diode model exhibiting transient behavior.

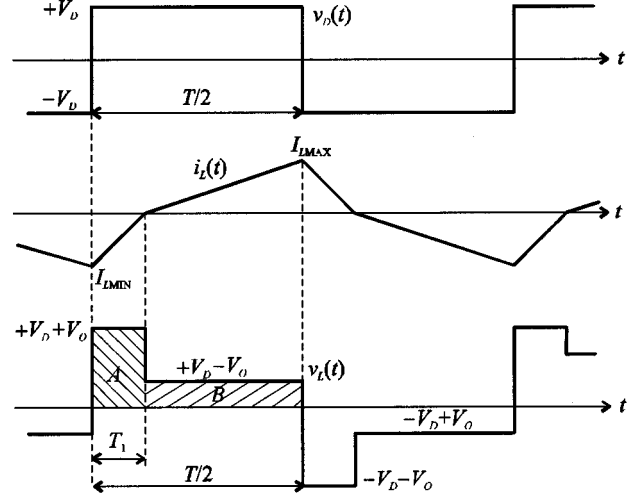


Fig. 8. Ideal operation of the rectifier in Fig. 1: drive, inductor current and inductor voltage waveforms.

Equation (1) shows that at a given inductance value L , the normalized output voltage depends on the drive frequency ($1/T$) and the load R_L . Figs. 9 and 10 show a family of curves for a range of parameter $a = 4L/R_L$. Fig. 9 shows that output voltage is never greater than V_D . Each curve has a value of a ten times larger than the adjacent curve, shifting it a decade higher in frequency. This is obvious from the equation as well.

Fig. 10 shows that the pulses' delay time T_1 is nearly constant for low frequencies, and is equal to the circuit time constant $\tau_L = L/R_L$. At high frequencies, T_1 decreases and approaches $T/4$.

III. OPERATION INCLUDING DIODE REVERSE RECOVERY

Next we analyze the circuit again, under the same assumptions as the ideal case but employing the PWL diode model of Fig. 7 instead of ideal diodes. Fig. 11 shows a model of the converter with D_1 and D_3 conducting. The diode forward voltages v_{D1} and v_{D3} are neglected in comparison with other circuit voltages v_D , v_L , and V_O . As expected, the voltage and current waveforms (Fig. 12) show that the diodes do not switch off when the inductor current becomes negative at $t = T_1$. They conduct for an additional interval ΔT needed for stored excess minority charge carriers to be removed from the diode (reverse recovery). The delay time of the bridge pulses is now equal to the period $T_2 = T_1 + \Delta T$. To determine the steady-state output voltage,

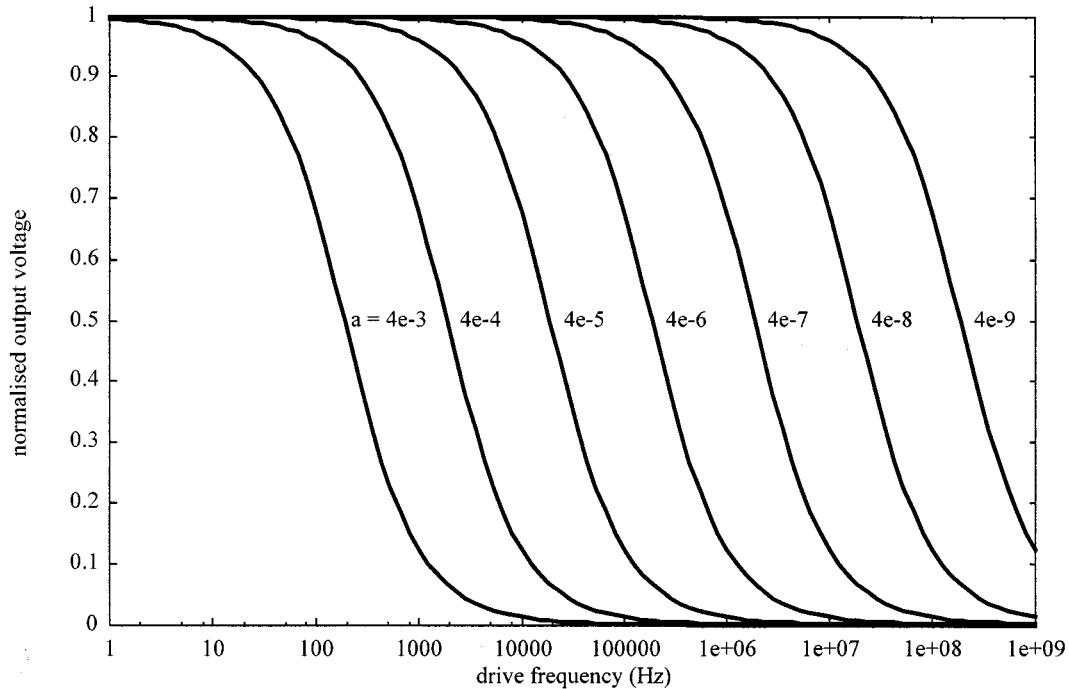


Fig. 9. Output voltage dependence on frequency for a wide range of parameter $a = 4L/R_L$.

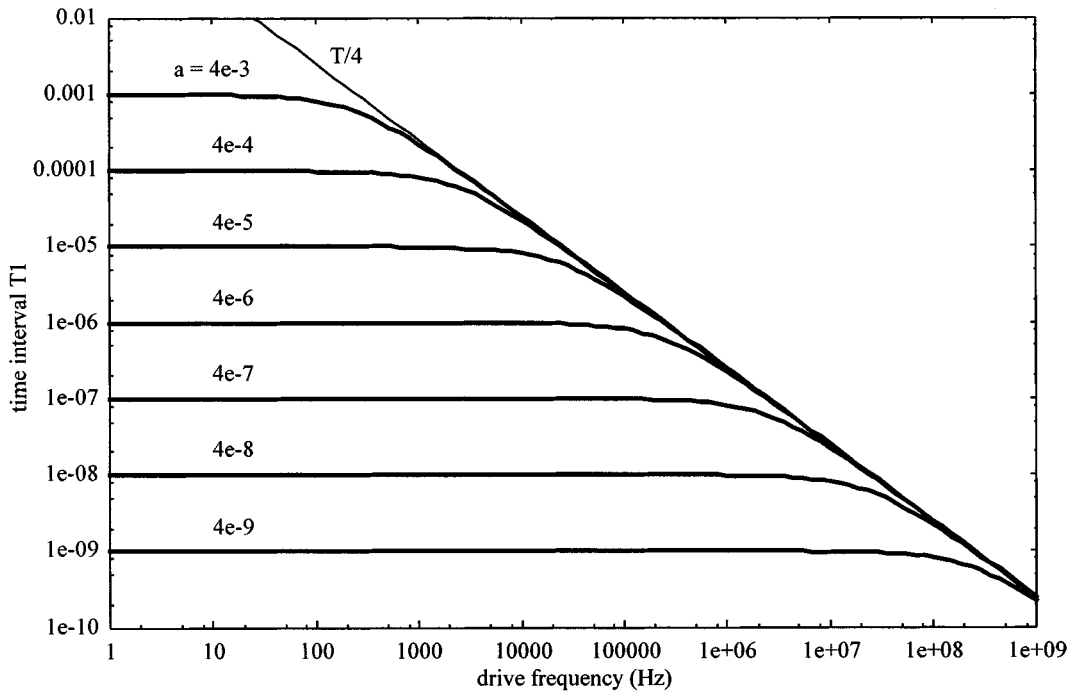


Fig. 10. Dependence on frequency of bridge pulses' delay time T_1 , for a wide range of parameter $a = 4L/R_L$.

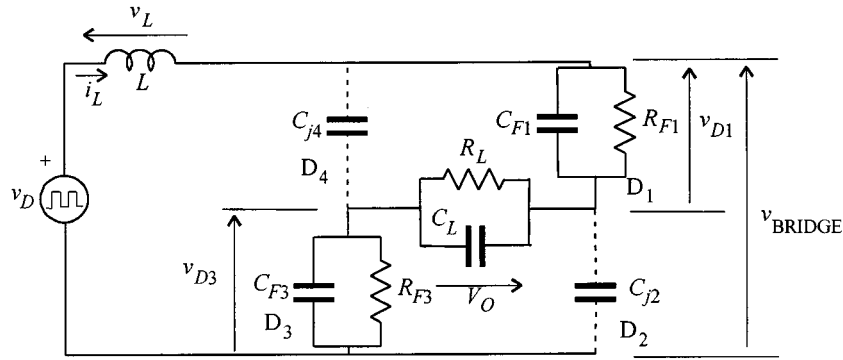
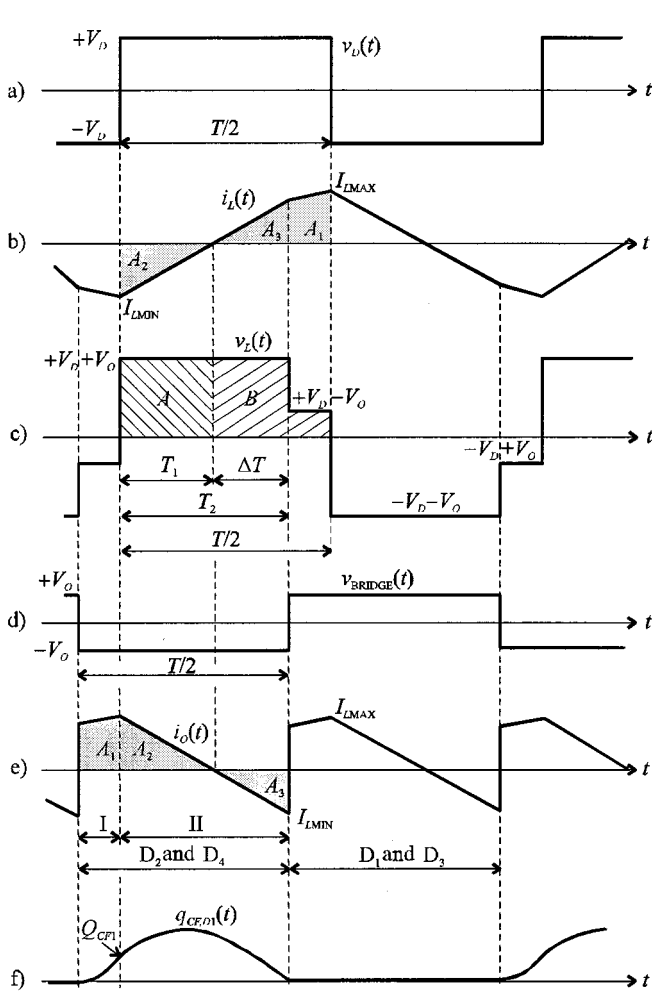
we need a system of three equations with three unknowns: either V_O , T_1 , and ΔT , or V_O , T_2 , and ΔT .

A. Qualitative Description

During the interval ΔT , negative current i_O flows through the output, discharging C_L [see area A_3 in Fig. 12(e)]. In the ideal case discussed in the Section II, the output current i_O was al-

ways positive. But now the negative part, area A_3 , lowers the average output current value. By equating the energy drawn from the drive source to that delivered to the load, we see that the output voltage must be higher with reverse recovery than in the ideal case (assuming the same drive frequency).

A rough comparison can be made by looking at the shaded areas under the current waveforms of Fig. 12(b) and (e). Average drive current during one half-cycle $I_{D(\text{half-cycle})}$ and output


 Fig. 11. Converter model with D_1 and D_3 conducting.

 Fig. 12. Operation including diode reverse recovery (case when V_O is lower than V_D): (a) drive voltage, (b) inductor current, (c) inductor voltage, (d) bridge voltage, (e) diodes' and output current, and (f) charge on diode-model capacitance C_F .

current I_O are proportional to the sum of the corresponding shaded areas: $I_{D(\text{half-cycle})} = 1/T(A_1 - A_2 + A_3)$ and $I_O = 1/T(A_1 + A_2 - A_3)$. Current I_O is larger than $I_{D(\text{half-cycle})}$ if $A_1 + A_2 - A_3 > A_1 - A_2 + A_3$, i.e., if $A_2 > A_3$.

Since these two areas are similar right-angled triangles, A_2 will be greater than A_3 if T_1 is greater than ΔT . When $\Delta T = T_1$, the two currents are the same, and $V_O = V_D$; when $\Delta T >$

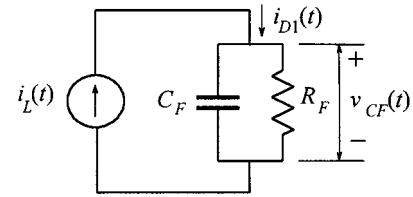


Fig. 13. Conducting diodes are driven by a linearly changing current source.

T_1 , I_O is less than $I_{D(\text{half-cycle})}$ and $V_O > V_D$. This explains the effect, perhaps surprising at first encounter, that diode reverse recovery increases the output voltage.

B. Quantitative Analysis

Unlike the ideal case, here, three equations are needed to determine the three unknowns in the steady state. The first two equations can be obtained in a similar manner as before. First, the symmetry of the waveforms about the time axis (see Fig. 12) makes $|i_L|$ at the end of each half-cycle equal (which also makes areas A and B equal)

$$\frac{V_D + V_O}{L} \cdot T_1 = \frac{V_D + V_O}{L} \cdot \Delta T + \frac{V_D - V_O}{L} \cdot \left(\frac{T}{2} - T_1 - \Delta T \right)$$

or

$$\frac{V_D + V_O}{L} \cdot (T_2 - 2 \cdot \Delta T) = \frac{V_D - V_O}{L} \cdot \left(\frac{T}{2} - T_2 \right). \quad (3)$$

The output stage gives the second equation

$$V_O = R_L \cdot I_O$$

where the current I_O can be obtained by averaging the diodes' current i_D

$$\begin{aligned} I_O &= \frac{1}{T/2} \int_0^{T/2} i_D d\tau \\ &= \frac{1}{T/2} \int_0^{T_2} \left(-\frac{V_D + V_O}{L} \tau + \frac{V_D + V_O}{L} T_1 \right) d\tau \\ &\quad + \int_{T_2}^{T/2} \left(\frac{V_D - V_O}{L} (\tau - T_2) + \frac{V_D + V_O}{L} \Delta T \right) d\tau. \end{aligned}$$

Solving the integrals and using (3) we obtain

$$I_O = \frac{V_D + V_O}{L} \cdot \frac{T_2}{T} \left(\frac{T}{2} - 2\Delta T \right)$$

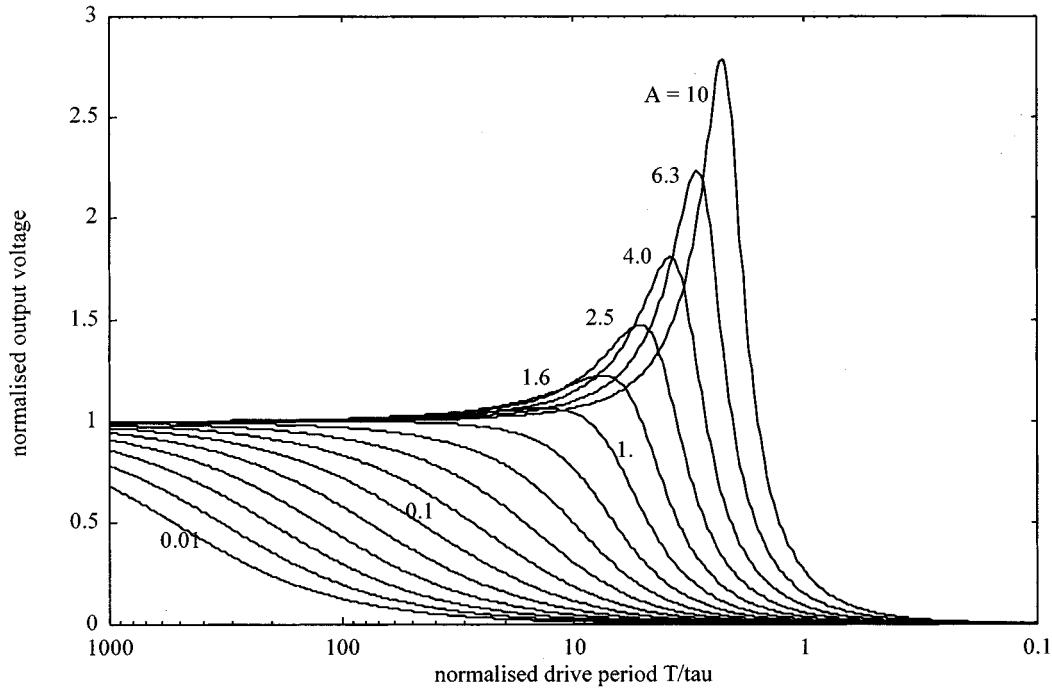


Fig. 14. Dependence of the normalized output voltage v on the normalized drive period T_n .

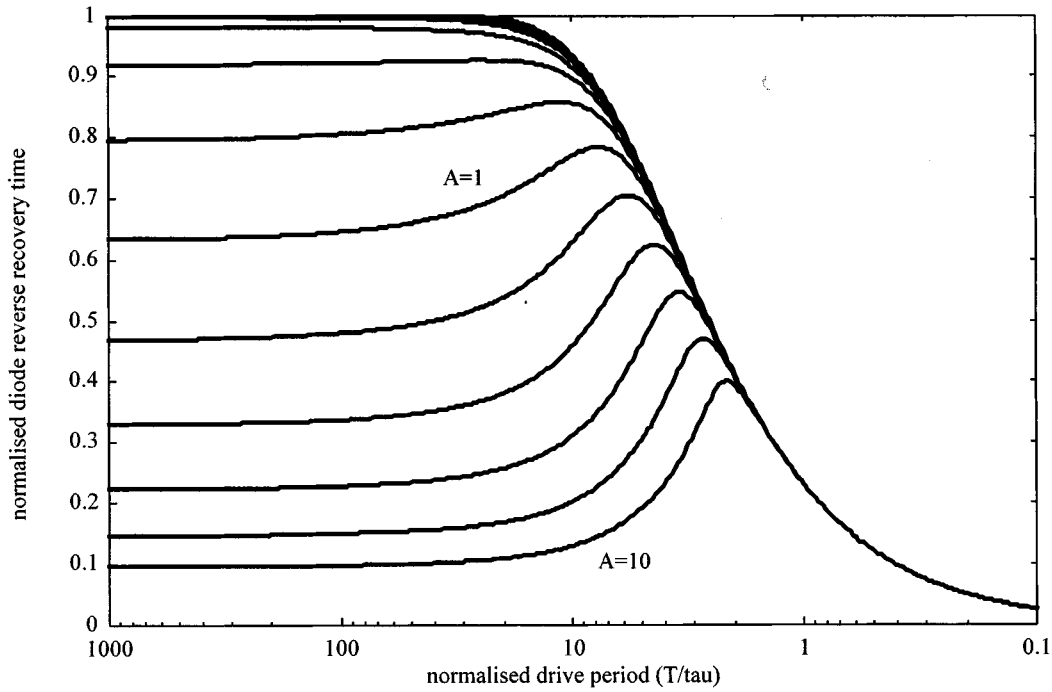


Fig. 15. Dependence of the normalized diode reverse-recovery time Δt on the normalized drive period T_n .

or

$$V_O = R_L \cdot \frac{V_D + V_O}{L} \cdot \frac{T_2}{T} \left(\frac{T}{2} - 2\Delta T \right). \quad (4)$$

Equations (3) and (4) can be transformed to obtain explicit relations for V_O and ΔT . From (3) we have

$$\Delta T = \frac{1}{2} \cdot \left[T_2 - \left(\frac{T}{2} - T_2 \right) \frac{V_D - V_O}{V_D + V_O} \right]. \quad (5)$$

Substituting ΔT in (4) and rearranging yields

$$\frac{V_O}{V_D} = 2 \cdot \frac{R_L}{L} \cdot \frac{T_2}{T} \left(\frac{T}{2} - T_2 \right). \quad (6)$$

The third equation is found from the diode reverse recovery. Since our simple PWL diode model contains only linear capacitances and a linear resistance (in contrast to exponentially nonlinear ones in real diodes), the analysis involves only a

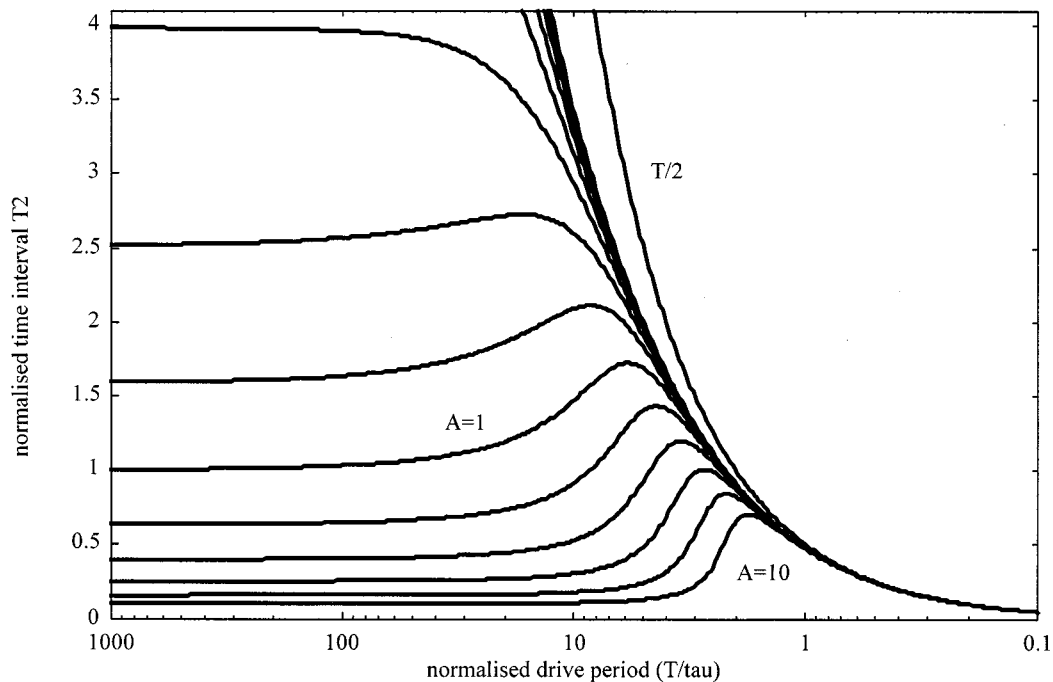


Fig. 16. Dependence of the normalized bridge pulses' delay time t_2 on the normalized drive period T_n .

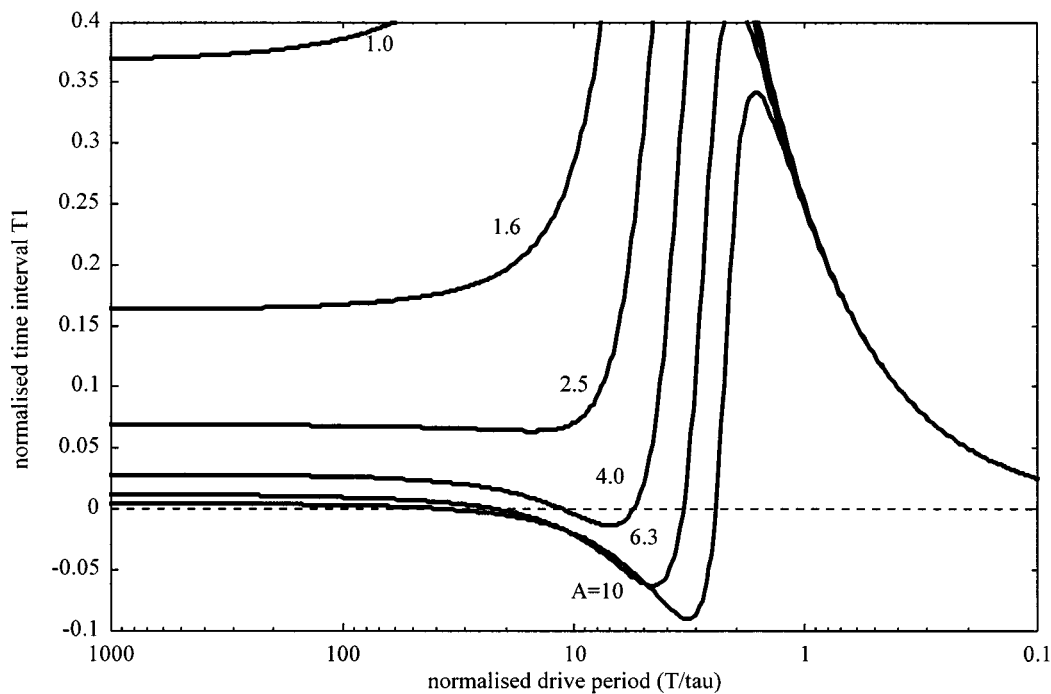


Fig. 17. Dependence of the normalized time interval t_1 on the normalized drive period T_n .

simple RC circuit. The junction capacitances of the nonconducting diodes are neglected, since they pass only a small current. The converter model comprises three RC circuits driven by a current source (inductor current), which changes linearly with time. Diode reverse recovery is determined by the charging and discharging of C_F , so we must analyze the $R_F C_F$ circuit of Fig. 13. Two intervals are involved,

shown in Fig. 12(e) and (f): the first lasts for $T/2 - T_2$, when $|di_L/dt| = (V_D - V_O)/L$; the second lasts for T_2 , when $|di_L/dt| = (V_D + V_O)/L$.

C. Interval I

The diode is switched on at the beginning of the first interval when C_F is empty. For a period $T/2 - T_2$ the $R_F C_F$ circuit

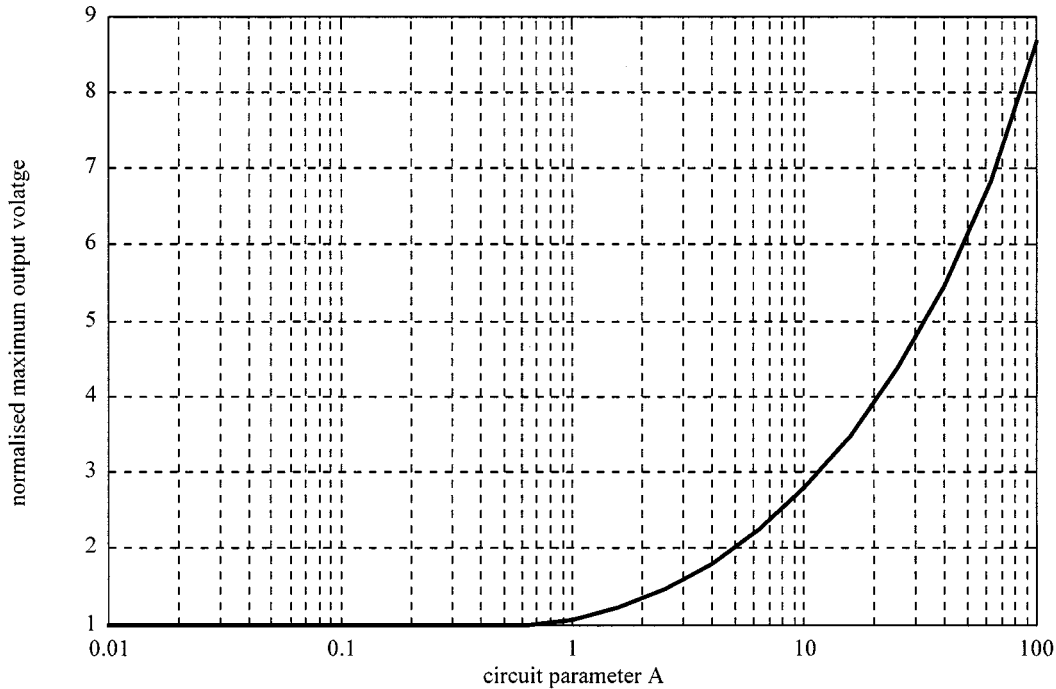


Fig. 18. Dependence of the maximum normalized output voltage on the parameter $A = \tau R_L/L$.

passes the inductor current, and the instantaneous value of the charge q_{CF} on C_F is

$$q_{CF}(t) = [q_{CF}(0^+) - q_{CFP}(0^+)] \exp(-t/\tau) + q_{CFP}(t)$$

where $q_{CF}(0^+) = 0$ is the initial charge immediately after the start of the interval ($t = 0$), $\tau = C_F R_F$ is the diode model time constant (representing excess minority charge carrier recombination time) and q_{CFP} is the particular solution of $C_F R_F$ circuit differential equation

$$q_{CFP}(t) = \tau \cdot i_{D1}(t - \tau).$$

Since we neglect current through the junction capacitances C_j of nonconducting diodes, i_{D1} is nearly equal to i_L . Bearing in mind that

$$i_{D1}(t) \approx i_L(t) = \frac{V_D - V_O}{L} t + \frac{V_D + V_O}{L} \Delta T$$

we obtain

$$q_{CFP}(t) = \tau \cdot \left[\frac{V_D - V_O}{L} (t - \tau) + \frac{V_D + V_O}{L} \Delta T \right]$$

and

$$q_{CFP}(0^+) = \tau \left(-\frac{V_D - V_O}{L} \tau + \frac{V_D + V_O}{L} \Delta T \right).$$

Finally, we get the instantaneous diode charge as

$$q_{CF}(t) = \frac{\tau}{L} \left\{ [(V_D - V_O)\tau - (V_D + V_O)\Delta T] \exp(-t/\tau) + (V_D - V_O)(t - \tau) + (V_D + V_O)\Delta T \right\}.$$

At the end of this interval ($t = T/2 - T_2$), the charge on C_F is

$$Q_{CF1} \frac{L}{\tau} = [(V_D - V_O)\tau - (V_D + V_O)\Delta T] \cdot \exp \left[-\left(\frac{T}{2} - T_2 \right) / \tau \right] + (V_D - V_O) \cdot \left(\frac{T}{2} - T_2 - \tau \right) + (V_D + V_O)\Delta T. \quad (7a)$$

D. Interval II

Now, following the same procedure and using $q_{CF}(0^+) = Q_{CF1}$ as an initial condition and a new time axis with the origin at the beginning of this interval, we have

$$i_{D1}(t) \approx i_L(t) = -\frac{V_D + V_O}{L} t + \frac{V_D + V_O}{L} T_1$$

$$q_{CFP}(t) = \tau \left[-\frac{V_D + V_O}{L} (t - \tau) + \frac{V_D + V_O}{L} T_1 \right]$$

$$q_{CFP}(0^+) = \tau \left(\frac{V_D + V_O}{L} \right) (T_1 + \tau)$$

and finally

$$q_{CF}(t) = \frac{\tau}{L} \left\{ \left[Q_{CF1} \frac{L}{\tau} - (V_D + V_O)(T_1 + \tau) \right] \exp(-t/\tau) - (V_D + V_O)(t - \tau) + (V_D + V_O)T_1 \right\}.$$

At the end of the second interval ($t = T_2$) the capacitance C_F is completely discharged, $q_{CF}(t) = 0$, and the diode switches off. Substituting $T_2 - \Delta T$ for T_1 , the previous equation becomes

$$0 = \left[Q_{CF1} \frac{L}{\tau} - (V_D + V_O)(T_2 - \Delta T + \tau) \right] \exp(-T_2/\tau) - (V_D + V_O)(\Delta T - \tau). \quad (7b)$$

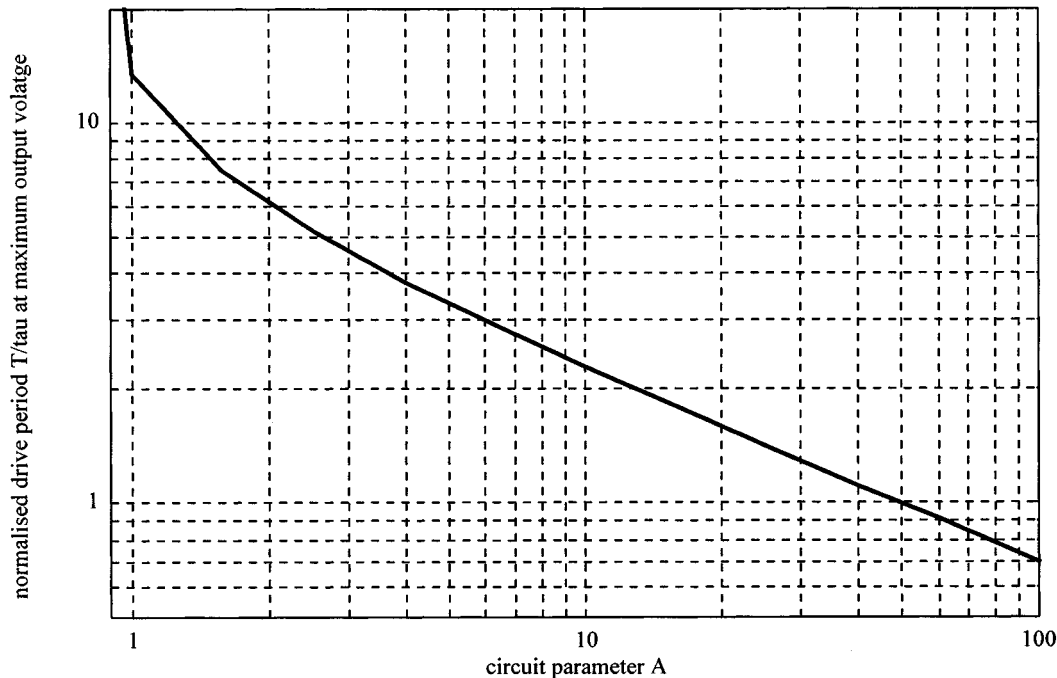


Fig. 19 Normalized drive period at maximum output voltage dependence on parameter $A = \tau R_L/L$.

The system of (5)–(7) can be normalized with respect to the drive voltage V_D and the diodes' excess minority carrier recombination lifetime τ (equal to $R_F C_F$ in the PWL diode model)

$$v = \tau \cdot \frac{R_L}{L} \cdot \frac{2t_2}{T_n} \left(\frac{T_n}{2} - t_2 \right) \quad (8)$$

$$\Delta t = \frac{1}{2} \cdot \left[t_2 - \left(\frac{T_n}{2} - t_2 \right) \frac{1-v}{1+v} \right] \quad (9)$$

0 =

$$[B - (1+v)(t_2 - \Delta t + 1)] \exp(-t_2) - (1+v)(\Delta t - 1) \quad (10a)$$

where

$$B = [(1-v) - (1+v)\Delta t] \exp\left(-\frac{T_n}{2} + t_2\right) + (1-v) \cdot \left(\frac{T_n}{2} - t_2 - 1\right) + (1+v)\Delta t. \quad (10b)$$

The normalized equations show that, out of eight circuit and diode parameters, only three qualitatively determine its behavior: inductance L , load resistance R_L , and diode excess minority charge carrier recombination time τ . All three appear only in the first equation, forming a constant that can be denoted by a parameter $A = \tau R_L/L$. This explains why the phenomenon can be observed experimentally even when fast diodes are used. If τ is small, the phenomenon appears at large R_L and/or small L . It appears at higher frequencies, since the drive period in equations is normalized by τ . For example, Fig. 6 was measured for $L = 9.42$ mH, $R_L = 10$ k Ω and $\tau = 7.2$ μ s, giving $A = 7.64$, and the maximum output voltage occurred at $f = 43$ kHz. Our model predicts a similar graph and behavior with faster diodes having $\tau = 1$ μ s but with

$L = 100$ μ H, $R_L = 764$ Ω , since these new parameters give the same $A = 7.64$. The maximum would then be at 7.2 times higher frequency, $f = 310$ kHz, since τ is that much smaller.

IV. NUMERICAL SOLUTION

The nonlinear system of equations can be solved numerically, using the Newton–Raphson method (or similar). The results are shown in Figs. 14–17.

Fig. 14 shows how the normalized output voltage depends on the normalized drive period. Unlike the ideal case in Fig. 9, where the normalized output voltage is always less than unity and decays monotonically with rising frequency, here, at higher A values, it becomes greater than unity, increases to a maximum, then decays more steeply toward zero. This agrees with the deviations noticed in practical converters, described above. The maximum value of the output voltage, and the frequency at which it occurs, depend on the parameter A . These functions, $v_{\text{MAX}} = f(A)$ and $f_{V_{\text{MAX}}} = f(A)$, can be determined by calculating $\delta v/\delta A$ and are shown in Figs. 18 and 19.

The numerical results are verified by comparison with experimental measurements. The experimental dependence shown in Fig. 6 was obtained for circuit parameters that give $A = 7.64$, and measurements give $v = 12.24/5 = 2.45$ and $T_n = 1/(43 \text{ kHz} \cdot 7.2 \text{ } \mu\text{s}) = 3.23$. The numerical results of Figs. 18 and 19 for the same A agree well: $v = 2.5$ and $T_n = 2.7$. This validates the simplifications made in the analysis.

As further validation, we compare the theoretical predictions with the experimental results of the dependence of the output voltage V_O on the load R_L . Fig. 20 was produced using the same circuit parameters as for Figs. 3 and 5: $v_D = \pm V_D = \pm 5$ V, $L = 9.42$ mH, $C_L = 61.5$ nF, and a constant operating frequency $f = 27$ kHz ($T = 37$ μ s). For ideal operation, i.e.,

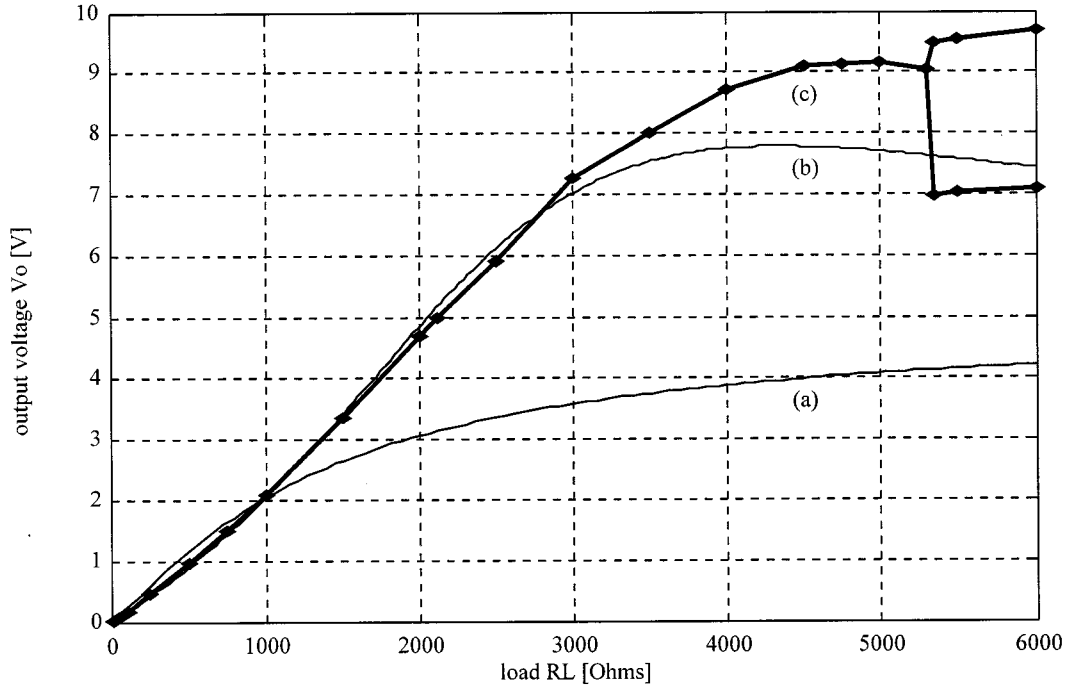


Fig. 20. Dependence of the output voltage V_O on the load R_L : (a) ideal operation, (b) theoretical predictions for diodes with $\tau = 7.2 \mu\text{s}$, and (c) experimental results with diodes MR 752.

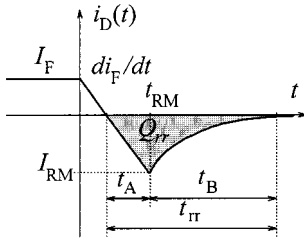


Fig. 21. Typical diode reverse recovery waveform during inductive current switching off.

using ideal diode model which includes no charge storage effects, curve (a) remains below $V_D = 5 \text{ V}$ for all loads. For diodes with $\tau = 7.2 \mu\text{s}$ (which gives a reverse recovery of $5 \mu\text{s}$), theoretical predictions give curve (b), and curve (c) presents experimental results with diodes MR 752. As the load resistance increases, the output voltage becomes higher than V_D at $R_L = 2050 \Omega$ on the theoretical nonideal curve (b) and at 2120Ω on the experimental curve (c). The curve (b) peaks to a value of 7.8 V at $R_L = 4330 \Omega$, while the curve (c) has a peak of 9.17 V at 5000Ω . The experimental results are in good agreement with the theoretical predictions, made using a very simple diode model. At load resistance higher than 5300Ω the experiments show that output voltage oscillates between two levels depicted by two lines in Fig. 20: the DH phenomenon. The steady state analysis presented here cannot describe this effect; it has a dynamic nature and is planned to be investigated in a future paper.

Figs. 15–17, respectively show the dependence of the normalized diode reverse recovery time Δt , the bridge pulse delay t_2 , and t_1 on the normalized drive period T_n . These dependencies are nonmonotonic. Moreover, since t_2 cannot increase further than $(T/2)/\tau$ when Δt increases with V_O , t_1 becomes nega-

tive (see Fig. 17) for certain frequencies. This interval occurs at frequencies below those giving maximum output voltage, and coincides with the appearance of the DH phenomenon. The two seem to be closely linked, and their connection will be presented in the future paper.

V. DESIGN CONSIDERATIONS

The parameter τ is an important quantity in the PWL diode model, but it is not generally given in device data sheets. However, it can be calculated from the reverse recovery information usually given. Fig. 21 shows a typical reverse recovery waveform and defines the quantities I_F , di_F/dt , and t_A . It can be shown that, if the negative diode current increases at a higher rate so that charge removal is accomplished before substantial recombination can occur [2] (the usual case reflected in diode data sheets published by most manufacturers)

$$t_A \approx \sqrt{\frac{2I_F\tau}{|di_F/dt|}} \quad \text{or} \quad \tau \approx \frac{|di_F/dt|}{2I_F} t_A^2.$$

If the temperature is increased, the reverse recovery of silicon P-i-N diodes is significantly degraded due to increased minority carrier charge storage effects. On the contrary, GaAs Schottky rectifiers have reduced reverse recovery at elevated temperature [10].

Figs. 14 and 18 show that the output voltage V_O becomes higher than the drive voltage V_D only when A becomes greater than unity (approximately). This overvoltage can be several times higher than V_D at higher A values, i.e., at light loads or with slow diodes, and might destroy output filter capacitors, usually designed for $V_O \leq V_D$. To avoid overvoltages and strange behavior, the series-resonant converter and high-fre-

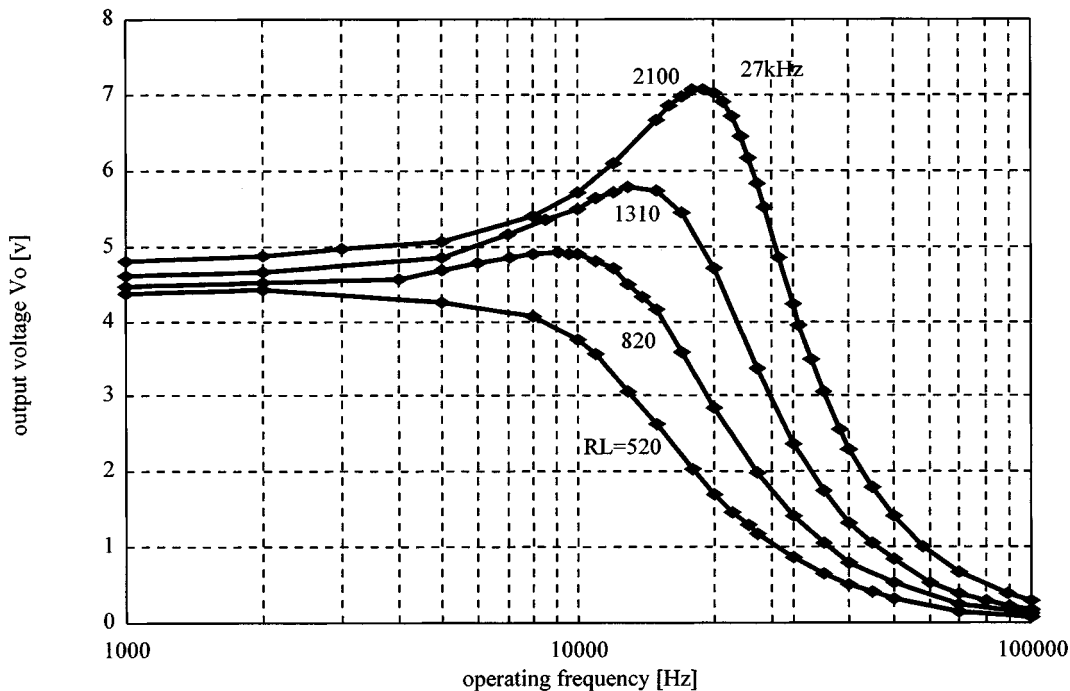


Fig. 22. Measured dependence of the output voltage on frequency for R_L values giving $A = 1.6, 1.0, 0.63,$ and 0.40 .

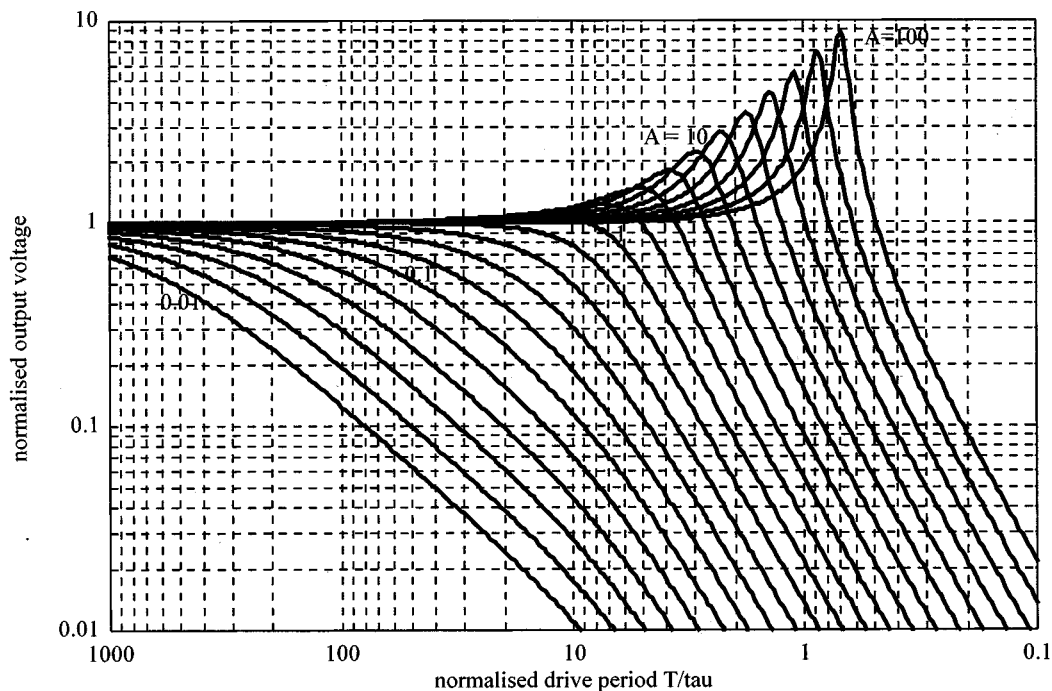


Fig. 23. Dependence of the normalized output voltage v on the normalized drive period T_n .

quency rectifiers should be designed so that even in the worst case, i.e., at lightest loads, the condition $A = \tau R_L/L < 1$ is satisfied, giving $L/R_{L,MAX} > \tau$.

For example, the parameters used for Figs. 6 and 20 give the circuit time constant $L/R_L = 9.42 \text{ mH}/10 \text{ k}\Omega = 0.942 \mu\text{s}$, the diode time constant $\tau = 7.2 \mu\text{s}$ and $A = 7.2/0.942 = 7.64$. To make A less than unity we need to increase L/R_L , by decreasing R_L , increasing L , or adjusting both simultaneously.

Fig. 22 shows the measured dependence of the output voltage on frequency for decreased R_L values giving $A = 1.6, 1.0, 0.63,$ and 0.40 . These curves agree well with the theoretical predictions from Fig. 14 and validate the above consideration.

If the circuit parameters are given, Fig. 14 and the above relation can be used to determine the maximum switching frequency above which the output voltage decreases below allowable limits, e.g., by 10% or less. (For this purpose, the voltage

axis of Fig. 23 employs a log scale for improved legibility.) On the other hand, if the switching frequency is known, Fig. 23 gives the minimum A value for the same criterion. Hence the maximum allowable inductance at the input of the bridge rectifiers can be determined. This condition should be met even for the worse case, i.e., for the minimum value of R_L .

The above relation is also useful for the series-resonant converter, since at high frequencies its behavior is similar (see Figs. 3 and 6). The relation should be added to the design rules for series-resonant converters [3, p. 405] and is a further reason for adding a preload at the output. Also, the correct frequency range for regulating the output voltage can be determined from Fig. 23.

VI. CONCLUSION

Diode reverse recovery affects the operation of high-frequency rectifiers. The deviations from ideal operation can produce substantial overvoltages and quasiperiodic oscillation, open-loop. The equations derived clearly show that the phenomena depend on $A = \tau R_L/L$, i.e., on only three out of eight circuit parameters. These are

- 1) diode excess minority charge carrier recombination time τ (which can be derived from data-sheet information);
- 2) converter load resistance R_L ;
- 3) source inductance L .

Comparison with experimental measurements shows close agreement. When faster diodes are used, the same effects will be observed but at higher frequencies.

An additional constraint, $A < 1$ or $L/R_{L,MAX} > \tau$, should be added to the design rules for converters, in order to protect the circuit from overvoltages (which might damage output filter capacitors) and from open-loop instability (quasiperiodicity). For frequency-controlled converters, a modified frequency range should be used, and this can be determined from the graphs presented.

The work presented here can be adapted for the analysis of similar phenomena in other converters. All switching converters have some stray inductance in series with their diodes, so we expect the phenomena to be widespread, especially as switching frequencies are pushed ever higher. Further investigations should explain the DH phenomenon and how it depends on circuit parameters; the general influence of delay; and similar effects in switching converters where the duty ratio is not 0.5. Analysis of appropriate control methods and their closed-loop stability are also of interest. These and other investigations are made possible now a suitable piecewise-linear diode model is available.

REFERENCES

- [1] B. K. Bose, *Power Electronics and Variable Frequency Drives: Technology and Applications*. New York: IEEE Press, 1996.
- [2] N. Mohan, T. M. Underland, and W. P. Robins, *Power Electronics: Converters, Applications and Design*, 2nd ed. New York: Wiley, 1995.
- [3] M. K. Kazimierczuk and D. Czarkowski, *Resonant Power Converters*. New York: Wiley, 1995.

- [4] J. G. Kassakian, M. F. Schlecht, and G. C. Verghese, *Principles of Power Electronics*. Reading, MA: Addison-Wesley, 1991.
- [5] R. L. Steigerwald, "A comparison of half-bridge resonant converter topologies," *IEEE Trans. Power Electron.*, vol. 3, pp. 174–182, Apr. 1988.
- [6] J. H. B. Deane and D. C. Hamill, "Instability, subharmonics, and chaos in power electronic systems," *IEEE Trans. Power Electron.*, vol. 5, pp. 260–268, July 1990.
- [7] L. V. Karadzinov, G. L. Arsov, and L. Kocarev, "Amplitude modulation phenomenon in series-resonant converters," in *Proc. 4th Theme ETAI Symp. Int. Participation*, Ohrid, Macedonia, Sept. 27–29, 1993, pp. 33–34.
- [8] L. V. Karadzinov, D. J. Jefferies, G. L. Arsov, and J. H. B. Deane, "Simple piecewise-linear diode model for transient behavior," *Int. J. Electron.*, vol. 78, no. 1, pp. 143–160, 1995.
- [9] G. L. Arsov and L. V. Karadzinov, "Influence of the circuit parameters on the DH phenomenon," in *Proc. 8th Symp. Power Electron.—Ee'95*, Novi Sad, Yugoslavia, Sept. 27–29, 1995, pp. 253–258.
- [10] C. R. Winterhalter, S. Pendharkar, and K. Shenai, "Modeling and characterization of reverse recovery performance of high-power GaAs Schottky and silicon P-I-N rectifiers," in *Proc. 26th Annu. IEEE Power Electron. Spec. Conf.—PESC'95*, vol. 2, Atlanta, GA, June 18–22, 1995, pp. 847–850.



Lúpeo Karadžinov (S'90–M'94) was born in Skopje, Macedonia, in 1963. He received the Dipl. Eng. degree in electronics and telecommunications from the Faculty of Electrical Engineering, Saints Cyril and Methodius University (SCMU), Skopje, in 1988 and the M.Sc. and Ph.D. degrees from the Faculty of Electrical and Computer Engineering, University of Zagreb, Croatia, in 1993 and 1999, respectively.

In 1989, he joined the staff of the Institute of Electronics, Faculty of Electrical Engineering, SCMU, as a Teaching and Research Fellow. He was a Visiting Researcher, funded by a British Council fellowship, from 1993 to 1994, in the Department of Electronic and Electrical Engineering, and in 1999, was with the Surrey Space Centre, both at the University of Surrey, U.K. He jointly initiated a European Commission project to introduce new undergraduate and postgraduate power electronics courses at SCMU. His research interest is in high frequency switching power converters, nonlinear dynamics and device modeling, where he has published more than 20 papers.

Dr. Karadzinov was the 1998 to 1999 Treasurer of the IEEE Republic of Macedonia Section. He is a Member of the International Federation of Automatic Control. He has been President of the Macedonian national section of the Young European Federalists (JEF) for four years.



David C. Hamill (M'89–SM'94) was born in London, U.K. He received the B.S. and M.S. degrees from the University of Southampton, Southampton, U.K., and the Ph.D. degree from the University of Surrey, Guildford, U.K.

After practicing as a Design Engineer and a Consultant, he was Technical Director of PAG Ltd., London, U.K., for seven years. In 1986, he joined the University of Surrey, where he is currently a Senior Lecturer in the Surrey Space Centre. His research interests include dc–dc conversion, space

power systems, nonlinear dynamics, and FACTS. He is the Contractor of a European Commission project to introduce new undergraduate and postgraduate power electronics courses at Saints Cyril and Methodius University, Skopje, Macedonia.

Dr. Hamill is a Member of the IEEE Technical Committee on computers in power electronics, a member of the IEE, and a Chartered Engineer. He was an Associate Editor of the IEEE TRANSACTIONS ON POWER ELECTRONICS from 1994 to 1996, and was on the Guest Editorial Panel of a special issue on computers in power electronics. He was the Guest Editor of a special issue on switched-mode dc power supplies in the *International Journal of Electronics*.